RSC Advances

ROYAL SOCIETY OF CHEMISTRY

www.rsc.org/advances

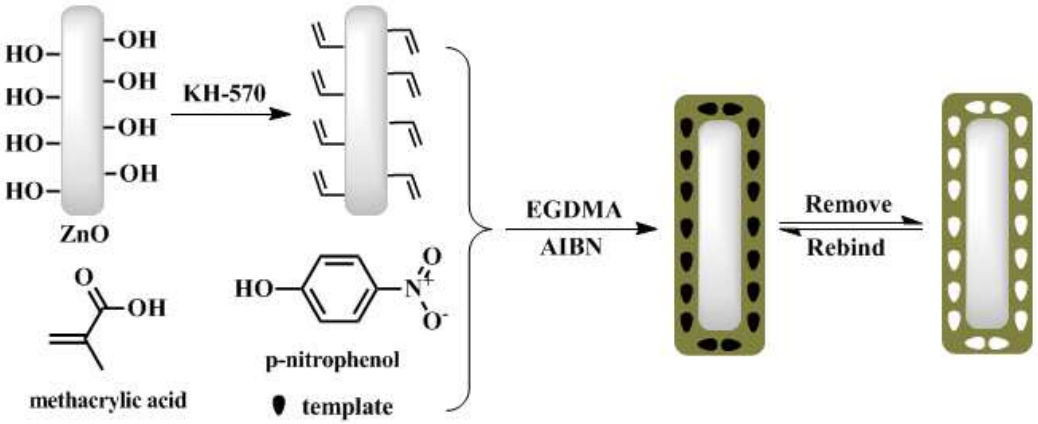

A novel MIPs-based ZnO nanorods with molecular recognition ability for paranitrophenol was successfully synthesized via a surface imprinting-directing polymerization.

A novel molecularly imprinted polymer thin film at surface of ZnO nanorods for selective fluorescence detection of Paranitrophenol

Xiao Wei,[a] Zhiping Zhou,[a] Tongfan Hao,[a] Hongji Li,[b] Yanzhuo Zhu,[c] Lin Gao,[b] Yongsheng Yan [b*]

[a]School of Material Science and Engineering, Jiangsu University, Zhenjiang 212013, China
[b]School of Chemistry and Chemical Engineering, Jiangsu University, Zhenjiang 212013, China
[c] School of the Environment, Jiangsu University, Zhenjiang 212013, China

ABSTRACT

Inspired by a surface imprinting-directing polymerization system, an effective and simple synthesis method was first developed to prepare an imprinted polymer thin film at the surface of ZnO nanorods (ZnO NRs), and the composites were used as fluorescence sensors for sensitively and selectively recognizing the target paranitrophenol (4-NP). The vinyl-modified ZnO NRs were used as the solid supports and optical materials. The obtained materials (MIPs-ZnO NRs), which were composed of ZnO NRs as fluorescence signal and MIPs as molecular selective recognition sites, could sensitively and selectively recognize the template molecules by using the spectrofluorometer. After the experimental conditions were optimized, a linear relationship was obtained covering the linear range of 0.5-14 μmol L^{-1} with a correlation coefficient of 0.9981. The developed method was applicable to routine trace determination of 4-NP in the spiked river water samples. This study provides a general strategy to fabricate imprinted polymer thin films-coated ZnO NRs with excellent performance for sensor application.

Keywords: ZnO nanorods, Fluorescence, Molecularly imprinted polymer thin film, Selective recognition, Paranitrophenol.

*Corresponding author at: School of Chemistry and Chemical Engineering, Jiangsu University, Zhenjiang 212013, PR China. Tel: +86 0511 88790683; fax: +86 0511 88791800.

E-mail address: jdwxtx@126.com

1 Introduction

Molecular imprinting is a well-established and powerful technique for synthesizing cross-linked polymer materials with tailor-made molecular recognition binding sites.[1] Its products, molecularly imprinted polymers (MIPs), are synthesized by the copolymerization of function monomers and a cross-linker in the presence of template molecules. After the removal of the template, the special tailor-made binding sites that are complementary to template molecules are obtained.[2] Due to the practicability, desired predetermination and specific selectivity, MIPs have been widely used in various significant applications, such as chemical sensor, separation, catalysis, drug delivery and so on.[1, 3-8] In recent years, surface molecular imprinting technique has been developed and explored due to the low binding kinetics, poor binding capacity and shortcomings of incomplete template removal from the bulk MIPs.[9, 10] Compared with the traditional method, this technique can provide a practical way to improve mass transfer and reduce permanent entrapment of the template by coating the MIPs film onto a solid support.[11] To date, due to the vast surface area, physical robustness and thermal stability, nanosphere and nanorod have been widely used in the surface imprinting process. [12]

As we know, functional MIPs have attracted great interest, including magnetic response (magnetic separation),[13] temperature response (enhanced rebinding percentage and mass transfer),[14] fluorescence characteristics (fluorescent recognition)[15] and so on. Among them, MIPs-based fluorescence sensors have been widely used for the determination of different substances, meanwhile, fluorescent recognition methods have been widely used as powerful techniques due to their low cost, rapid response, low detection limit, and high sensitivity.[16] For example, Wang's group has reported the surface molecular imprinting on 1-vinyl-3-octylimidazolium ionic liquid-modified CdSe/ZnS QDs for optosensing of tocopherol.[17] Zhang's group has introduced a fluorescence nanosensing material by anchoring the MIPs layer on the surface of CdTe quantum dots for detecting cytochrome c.[18] Our group has prepared molecularly imprinted silica nanospheres

embedded mercaptosuccinic acid-coated CdTe QDs for selective recognition of λ-cyhalothrin and reported a facile and general method for preparing an imprinted polymer thin shell with Mn-doped ZnS QDs at the surface of silica nanoparticles for detecting 2,4-dichlorophenol.[15, 19] However, up to now, most of studies focus on the MIPs-QDs (CdSe, CdTe and ZnS) sensor, ignoring some helpful optical materials, such as ZnO. ZnO is a wide-band-gap semiconductor material with a large excitation binding energy at room temperature.[20] Due to the environmental friendliness and high chemical stability, composites combining ZnO with MIPs are hoped to sensitively and selectively detect analytes.

Nitrophenols, as a group of phenolic compounds, have been widely used in herbicide, pesticide, antiseptic and pharmacy. Nitrophenols have been listed by the U.S. Environmental Protection Agency (U.S.EPA) as priority environmental pollutants.[21, 22] Paranitrophenol (4-NP), one of the nitrophenol compounds, has raised worldwide concerns regarding public security and environmental problems because of its wide production and use by the medical and in agriculture. Thus, the detection of 4-NP from complex matrix is of great importance. To date, there have been a lot of methods reported such as high performance liquid chromatography (HPLC),[23, 24] electrophoresis and electrochemical methods,[25, 26] and chromatographic techniques[27] for the determination of 4-NP. However, the shortcomings of these methods are: time consuming, expensive reagents and tedious sample pretreatment. Therefore, the development of simple, rapid and selective 4-NP detecting methods presents a challenge.

In this work, we made a first attempt to prepare an imprinted polymer thin film based FL sensor by using vinyl-modified ZnO NRs as the solid supports and optical materials via a surface imprinting-directing precipitation polymerization method. This imprinting thin film was obtained also using methacrylic acid (MAA) as the functional monomer, ethyl glycol dimethacrylate (EGDMA) as the cross-linker and 2,2'-azobisisobutyronitrile (AIBN) as the initiator. The as-synthesized nanomaterials were then used for selective recognition and FL detection of the target 4-NP. The MIPs-ZnO NRs were characterized by transmission electron microscope (TEM),

scanning electron microscope (SEM), X-ray diffraction (XRD) and Fourier transform infrared spectroscopy (FTIR). The FL quenching relationship between MIPs-ZnO NRs and 4-NP was investigated. This proposed FL imprinted polymer thin film artificial sensor (MIPs-ZnO NRs) aims to offer a simple, rapid and selective sensing system for detecting 4-NP in real samples.

2 Experimental

2.1 Materials and chemicals

Zinc acetate, KOH, 3-(methacryloyloxy)propyl trimethoxysilane (KH-570), methacrylic acid (MAA), ethyleneglycol dimethacrylate (EGDMA), 2,2'-azobis (2-methylpropionitrile) (AIBN) and paranitrophenol (4-NP), 2,4-dichlorophenol (2,4-DCP), 2,6-dichlorophenol (2,6-DCP), 2,4,5-trichlorophenol (2,4,5-TCP) were purchased from Aladdin reagent Co., Ltd. (Shanghai, China). Methylbenzene, acetonitrile, methanol and ethanol were purchased from Sinopharm Chemical Reagent Co.,Ltd. (Shanghai, China). All chemicals were of analytical grade reagents. Double distilled water (DDW) was used throughout the experimental procedures.

2.2 Instrument

The structure and morphology of the ZnO NRs and MIPs-ZnO NRs were observed by transmission electron microscope (TEM, JEOL, JEM-2100) and scanning electron microscope (SEM, JEOL, JSM-7001F). The X-ray diffraction (XRD) spectra were collected on a XRD-6100Lab X-ray diffractometer (Shimadzu, Japan) with Cu Kα radiation over the 2θ range of 10-80°. Infrared spectra (4000–400 cm^{-1}) were recorded using Nicolet NEXUS-470 FTIR apparatus (USA). The fluorescence measurements were performed on a Cary Eclipse spectrofluorometer (USA) equipped with a plotter unit and a quartz cell (1.0 cm × 1.0 cm). The Water bath oscillator is THZ-82A (Changzhou China).

2.3 Synthesis and Functionalization of ZnO NRs

ZnO NRs were prepared according to the reported method with minor modification.[28] In a typical synthesis, 7.5 g of zinc acetate was dispersed with methanol in a flask and the mixture was refluxed at 70 ^{o}C. When the solid was dissolved thoroughly, 30 mL of methanol containing 3.5 g of KOH was added into the solution. Then the solution was vigorous stirred for 3 days. After that, the products were collected by centrifugation and washed with ethanol several times to remove the unreacted reactants. Finally, the obtained ZnO NRs were dried in vacuum oven at 60 ^{o}C overnight.

The surface of ZnO NRs was endowed with reactive vinyl groups through modification with KH-570. Briefly, 1.0 g of ZnO NRs and 3.0 mL of KH-570 were dispersed in 50 mL of methylbenzene in a flask and vigorously stirred under N_2 at 90 °C for 12 h. The products were gathered with the help of high-speed centrifugation (12000 rpm, 5 min) and washed with DDW and ethanol three times to remove the unreacted reactant. Finally, the vinyl-modified ZnO NRs were dried under vacuum for further use.

2.4 Synthesis of MIPs-ZnO NRs

The molecularly imprinted polymer thin films at surface of ZnO NRs (MIPs-ZnO NRs) were prepared via a surface imprinting-directing precipitation polymerization method. Typically, 0.05 mmol of 4-NP, 0.2 mmol of MAA and 0.8 mmol of EGDMA were dissolved in 50 mL acetonitrile to self-assemble at room temperature. 50 mg of KH-570-ZnO NRs were dispersed into the above solution by ultrasonication. Then 10 mg of AIBN as the initiator was added and the mixture was purged with N_2 for 30 min. After that, the reaction was carried out in a water bath oscillator with a speed of 180 rpm by a two-step-temperature polymerization. The slow pre-polymerization was first undertaken at 50 ^{o}C for 6 h and the cross-linking polymerization was completed at 60 ^{o}C for 24 h. After the reaction, the products (MIPs-ZnO NRs) were collected with the help of high-speed centrifugation (12000 rpm, 5 min) and washed with ethanol several times to remove the unreacted monomers. The size and morphology of the MIPs thin films were controlled by changing the total amount of monomers. The template 4-NP

in the MIPs-ZnO NRs was extracted with a mixture solvent of methanol and acetic acid (9:1, v/v). The nonimprinted polymers (NIPs-ZnO NRs) were also prepared under the same conditions but without addition of 4-NP.

2.5 Measurement Procedure.

In the experiments, all the fluorescence detections were performed under the same conditions: the slit widths of the excitation and emission were both 10 nm. The excitation wavelength for fluorescence detection was set at 330 nm with a recording emission range of 350-450 nm and the value of photomultiplier tube voltage was set as 600 V. MIPs-ZnO NRs and NIPs-ZnO NRs were dispersed in DDW to get the fresh-made stock solution (200 mg/L). 4-NP stock solution (1.0 mmol/L, in DDW) was stocked at 4 ^{o}C. An appropriate quantity of MIPs-ZnO NRs or NIPs-ZnO NRs was added to a 5.0 mL comparison tube and a given concentration of analyte standard solution was added sequentially. Then, the mixture was diluted to volume with DDW and mixed thoroughly. After a certain time, a portion of the solution was transferred into a quartz cell and the fluorescence measured.

3 Results and discussion

3.1. Preparation and characterization of MIPs-ZnO NRs

The schematic illustration of preparing MIPs-ZnO NRs is shown in Figure 1. The MIPs-ZnO NRs were synthesized by a surface imprinting-directing precipitation polymerization method. In brief, ZnO nanorods were first prepared by a reflux mothod. Then, the ZnO NRs were functionalized with KH-570 via a simple silanization reaction to form polymerizable vinyl groups. In the next polymerization process, the vinyl-modified ZnO NRs were used as the solid supports and optical materials. Moreover, MAA, 4-NP, EGDMA and AIBN were used as the functional monomer, template, cross-linking agents and initiator, respectively. The imprinted polymer thin film was synthesized by a stepwise precipitation polymerization via the slow prepolymerization at 50 ^{o}C and the normal polymerization at 60 ^{o}C. After the

templates were removed from the imprinted polymers with solvent extraction, the MIPs-ZnO NRs were obtained and the recognition sites could selectively rebind the template molecules due to the good compatibility of size, shape and chemical interactions. The imprinted polymer thin film can further facilitate the template removal and maintain the excellent optical performance of the ZnO NRs.

Figure 1 Schematic illustration for the preparation of MIPs-ZnO NRs

The morphologies of ZnO NRs and MIPs-ZnO NRs were observed by TEM and SEM, which are shown in Figure 2 and Figure 3. In the synthesizing process of ZnO NRs, time is a critical factor and the colloids must be kept at 65 °C for at least 72 hours. As shown in Figure 2a, if the reaction time was insufficient, the NRs could not form. When the reaction time was enough, it could be found from the Figure 2b that the NRs were formed with a narrow size distribution and perfect surface structures. Moreover, From the TEM images, the size of the ZnO NRs could be also observed (the length is 80-100 nm and the diameter is 8.5-12.5 nm). As shown in Figure 2c and 2d, the ZnO NRs were wrapped by a very, very thin polymer film and the thickness of the film was about 2-3 nm. The sizes are listed in Table S1 in detail. It was obviously that the MIPs-ZnO NRs were highly claviform with a smooth surface, which is totally different from the short and straight feature of ZnO NRs. Due to the obvious aggregation of the ZnO NRs, the polymer film always tightly surrounded aggregation of the ZnO NRs. As soon as the amounts of the monomers changed significantly (0.3 mmol of MAA and 1.2 mmol of EGDMA), the homogeneous polymer film would be replaced by the irregular polymer layer (see in Figure S1), which affects directly identification effect. The results of SEM (see Figure 3) observations of the ZnO NRs and MIPs-ZnO NRs are consistent with TEM. As shown in Figure 3a and 3b, compared with the straight feature of ZnO NRs (Figure 3a), the SEM image of MIPs-ZnO NRs (Figure 3b) exhibits that the products are worm-like shapes after the

polymerization.

Figure 2 TEM images of ZnO NRs with insufficient reaction time (36 hours) (a) and sufficient reaction time (72 hours) (b), TEM images(c) and High resolution TEM images (d) of MIPs-ZnO NRs.

Figure 3 SEM images of ZnO NRs and MIPs-ZnO NRs.

Figure 4 displays the X-ray diffraction pattern of the MIPs-ZnO NRs, and for a comparison, the X-ray diffraction pattern of ZnO NRs is also shown (the inset in Figure 4). In the 2θ range of 10−80°, eleven characteristic peaks were indexed as (100), (002), (101), (102), (110), (103), (200), (112), (201), (004) and (440), respectively. The XRD pattern of MIPs-ZnO NRs was similar to that of ZnO NRs, indicating that the surface modification and grafting of polymer did not change the crystalline structure of ZnO NRs. In the 2θ range of 20-25°, there is a weak peak in the XRD pattern of MIPs-ZnO NRs, which is a little different from the XRD pattern of ZnO NRs, due to the imprinted polymer thin film coated the ZnO NRs.

Figure 4 XRD pattern of MIPs-ZnO NRs. For a comparison, the XRD pattern of ZnO NRs was included (inset).

The FT-IR spectra of ZnO NRs, KH-570-ZnO NRs, MIPs-ZnO NRs and NIPs-ZnO NRs were measured and shown in Figure 5a and 5b, respectively. As shown in Figure 5a, compared with the spectra of ZnO NRs (curve 2), KH-570-ZnO NRs (curve 1) displayed the characteristic peak at 1711 cm^{-1}, which might attribute to C=O

stretching vibration of KH570, indicating that the surface of the ZnO NRs was successfully endowed with reactive vinyl groups through modification with KH570. [29] As shown in Figure 5b (curve 1 and curve 2), MIPs-ZnO NRs and NIPs-ZnO NRs showed similar locations and appearance of the major bands. The three characteristic peaks at 1730 cm^{-1} (C=O stretching), 1257, and 1160 cm^{-1} (C−O−C stretching) affirmed the presence of EGDMA in the polymer thin film.[30] The characteristic peak at 1603 cm^{-1} are attributed to the stretch of C=C band, indicated that not all of the bonded EGDMA molecules were cross-linked.[31] The peak around 2968 cm^{-1} is C–H band, the characteristic peak at 1456 cm^{-1} is attributed to CH_3 band, and the absorption band at 3437 cm^{-1} (O–H stretching) of the polymer thin film could be attributed to MAA molecules. All those bands showed that the MIPs were grafted on the surface of the ZnO NRs.

Figure 5 FT-IR spectra of KH-570-ZnO NRs (a; curve 1), ZnO NRs (a; curve 2), MIPs-ZnO NRs(b; curve 1) and NIPs-ZnO NRs(b; curve 2).

3.2 Effect of the concentration of MIPs-ZnO NRs

To our knowledge, the amounts of MIPs-ZnO NRs had an obvious effect on the quenching efficency. Too low of an amount of MIPs-ZnO NRs would lead to a narrow linear range, whereas too high of an amount of MIPs-ZnO NRs would in too low of a sensitivity. Both linear range and detection sensitivity are important for the FL detection system. Therefore, the concentration of MIPs-ZnO NRs from 6.0 mg/L to 16 mg/L was used to study the effects on the 4-NP detection system ($C_{4\text{-NP}}$: 4.0 μmol/L). As shown in Figure 6, by changing the concentration of MIPs-ZnO NRs from 6.0 to 16 mg/L, the optimum value was 12 mg/L. As a result, the concentration of MIPs-ZnO NRs was fixed at 12 mg/L throughout the work.

Figure 6 Effects of the concentration of MIPs-ZnO NRs on FL intensity. Curve a: the

function of variation rate of FL intensity of detection system (containing MIPs-ZnO NRs + 4.0 μmol/L 4-NP) vs. concentration of MIPs-ZnO NRs; Curve b: the function of relative FL intensity vs. concentration of MIPs-ZnO NRs

3.3 Stability and Detection time

Before the performance testing, it was necessary to determine the optimal detection time. Firstly, it was expected to confirm the fluorescence stability of the MIPs-ZnO NRs without any templates. A solution which only contained MIPs-ZnO NRs with the concentration of 12 mg L^{-1} was estimated by the repeated detection of the fluorescence intensity every 10 min, as shown in Figure 7a. The fluorescence intensity of MIPs-ZnO NRs was stable for 7 times measurements within 60 min and the stability didn't change along with the time going. It was reflected that the MIPs-ZnO NRs could be contained stability for a long time under the condition. The maintained fluorescence intensity within 60 min may well be because the ZnO NRs were well protected by the polymer shell of the MIPs. To determine the optimal detection time, a certain amount of 4-NP (4.0 μmol/L) was mixed with MIPs-ZnO NRs (12 mg/L), the FL intensities were recorded at different interval time. As shown in Figure 7b, the relative intensity (F_0/F) increased at the initial beginning, when time was up to 9.0 min, the relative intensity was almost the same. Therefore, 9.0 min was selected as the optimal detection time for the following experiments.

Figure 7 Stabilities of MIPs-ZnO NRs (a) and Study of response time of 4-NP onto MIPs-ZnO NRs via FL detection (b).

3.4 MIPs-ZnO NRs and NIPs-ZnO NRs with template 4-NP of different concentrations.

In this test, under the optimal conditions, our aim was to demonstrate the recognition ability of the MIPs-ZnO NRs versus that of the NIPs-ZnO NRs (Figure 8).

MIPs-ZnO NRs were used as the optical materials to detect 4-NP based on the FL quenching between ZnO NRs and the target 4-NP, and NIPs-ZnO NRs were used as a contrast. The assay was implemented in a comparison tube with water after incubation target 4-NP with MIPs-ZnO NRs or NIPs-ZnO NRs for 9.0 min at room temperature. Figure 8a and 8b showed the spectral response of MIPs-ZnO NRs (12 mg/L) and NIPs-ZnO NRs (12 mg/L) with template 4-NP at different concentrations, respectively. The relationship between the FL intensity and the concentration of quenching 4-NP could be described by the Stern-Volmer equation:

$$F_0/F=1+K_{sv}[c] \quad (1)$$

F and F_0 are the FL intensities of the MIPs-ZnO NRs and NIPs-ZnO NRs at a given related 4-NP concentration and in a 4-NP free solution, respectively. K_{SV} is the Stern-Volmer quenching constant, and [c] is the concentration of 4-NP. The equation was applied to quantify the different quenching constants in this study and the ratio of $K_{SV,MIP}$ to $K_{SV,NIP}$ was defined as the imprinting factor (IF). As shown in Figure 8c, the $K_{SV,MIP}$ was found to be 197440 M^{-1} and the linear range of the calibration curve was 0.5-14 μmol L^{-1} with a correlation coefficient of 0.9981. As a control experiment, the FL response of NIPs-ZnO NRs to the 4-NP was investigated. As shown in Figure 8d, it could be found that the $K_{SV,NIP}$ was 33360 M^{-1}, the linear range of 2,4-DCP was also 0.5-14 μmol L^{-1} but with a correlation coefficient of 0.9973. Under this condition, the imprinting factor was 5.918, indicating that the MIPs-ZnO NRs had a better selectivity than the NIPs-ZnO NRs. The detection limit (3σ/k) was 0.036 μmol/L, in which k is the slope of the calibration line and σ is the standard deviation of blank measurements (n=11). It could be found that MIPs-ZnO NRs showed good selectivity but low sensitivity. This could be because of the inherent property for MIP@ fluorescent material detection systems. So there is a need to be done to improve the sensitivity of the MIPs-ZnO NRs in the future works.

As we know, reproducibility is an important factor for the imprinted nanomaterials. The reproducibility of the MIPs-ZnO NRs was studied at a fixed 4-NP concentration of 10 μmol L^{-1} and three repeated measurements were implemented with three MIPs-ZnO NRs under the same experimental conditions. After the assay, an

acceptable relative standard deviation (RSD) of 4.3% was obtained.

Figure 8 FL emission spectra of MIPs-ZnO NRs (a) and NIPs-ZnO NRs (b) (12 mg/L) with addition of the indicated concentrations of 4-NP in water solution and the Stern−Volmer plots for MIPs-ZnO NRs (c) and NIPs-ZnO NRs (d).

3.5 Selectivity.

When the 4-NP was removed by solvent extraction, imprinted binding sites were left in the polymer thin films that selectively bound the target 4-NP molecules. Several kinds of phenols, namely, 4-NP, 2,4-DCP, 2,6-DCP, 2,4,5-TCP were involved to evaluate the selectivity of MIPs-ZnO NRs. As shown in Figure 9, MIPs-ZnO NRs had a strong response to 4-NP, which caused a significant change of FL intensity with a high quenching amount. And the change in FL intensity of the MIPs based on ZnO NRs for 4-NP was more obvious than other phenols. By calculation, the difference in the quench amount (F_0/F-1) of MIPs-ZnO NRs and NIPs-ZnO NRs were 1.55, 0.09, 0.105, 0.095 at 10 μmol L^{-1} for 4-NP, 2,4-DCP, 2,6-DCP, 2,4,5-TCP, respectively. The results suggested that MIPs-ZnO NRs were specific to 4-NP but nonspecific to other phenols and there were no selective recognition sites in the NIPs-ZnO NRs. This result can be reasonably explained as follows: In the process of synthesis of the MIPs-ZnO NRs, many specific imprinted cavities with the memory of the template 4-NP were generated and the template could be bound strongly to the imprinted particles and caused changes in the FL intensity.

Figure 9 Quenching amounts of MIPs-ZnO NRs and NIPs-ZnO NRs by different kinds of 10 μmol L^{-1} phenols (4-NP, 2,4-DCP, 2,6-DCP, 2,4,5-TCP).

3.6 Analytical applications in Yangtze River sample

To demonstrate the applicability of this method, MIPs-ZnO NRs were used for 4-NP detection in Yangtze River water samples. The samples were filtered through 0.45 μm Supor filters and stored in glass bottles. As no phenols in Yangtze River samples were detectable by the proposed method, a recovery study was carried out and the corresponding results were listed in Table 1. The samples spiked with 0.5-12 μmol L^{-1} 4-NP were tested by MIPs-ZnO NRs, focusing on a "standard" curve which was obtained in the previous work (Figure 8c). According to this curve and the FL recovery measured values for the unkown samples, we were able to calculate the estimates of 4-NP levels in the water sample collected from Yangtze River. The recoveries were from 93.8% to 105.3%. The values determined by the MIPs-ZnO NRs show the excellent recognition ability to provide accurate numerical values of 4-NP concentrations on unknown environmental samples. Therefore, the MIPs-ZnO NRs could be regarded as an optional scheme for the rapid and direct analysis of relevant real samples.

Table 1 Recovery of 4-NP in Yangtze River samples with 4-NP solution at different concentration levels (n=5)

4 Conclusions

In summary, we have developed a surface imprinting-directing polymerization method for preparing an imprinted polymer thin film at the surface of ZnO NRs to obtain a new fluorescence composite sensor for FL detection and selective recognition of 4-NP from water medium. The vinyl-modified ZnO NRs were used as the solid supports and optical materials. Due to the high selectivity of MIPs and the strong fluorescence property of ZnO NRs, MIPs-ZnO NRs demonstrated highly selective and sensitive recognition and determination of 4-NP. Under optimum conditions, this special FL sensor was successfully applied to routine trace determination of 4-NP in the spiked river water sample. Furthermore, molecular recognition of MIPs-ZnO NRs is progress in our laboratory, which should generate tremendous interest due to its

great flexibility and versatility for future applications.

Acknowledgments

This work was financially supported by the National Natural Science Foundation of China (No. 21107037, No. 21176107, No. 21174057, No. 21277063, No. 21407057 and No. 21407064), National Basic Research Program of China (973 Program, 2012CB821500), Natural Science Foundation of Jiangsu Province (No. BK2011461, No. BK2011514 and No. BK20140535), Ph.D. Innovation Programs Foundation of Jiangsu Province (No. KYLX_1032), National Postdoctoral Science Foundation (No.2013M530240 and No. 2014M561595), Postdoctoral Science Foundation funded Project of Jiangsu Province (No. 1202002B and No. 1401108C) and Programs of Senior Talent Foundation of Jiangsu University (No. 12JDG090).

References

[1] S.F. Xu, J.H. Li, L.X. Chen, Molecularly imprinted core-shell nanoparticles for determination of trace atrazine by reversible addition-fragmentation chain transfer surface imprinting, J. Mater. Chem. 2011, 21, 4346.

[2] W. Lian, S. Liu, J. Yu, X. Xing, J. Li, M. Cui, J. Huang, Electrochemical sensor based on gold nanoparticles fabricated molecularly imprinted polymer film at chitosan–platinum nanoparticles/graphene–gold nanoparticles double nanocomposites modified electrode for detection of erythromycin, Biosensors and Bioelectronics 2012, 38, 163.

[3] X. Wei, Z.P. Zhou, T.F. Hao, H.J. Li, Y.S. Yan, Molecularly imprinted polymer nanospheres based on Mn-doped ZnS QDs via precipitation polymerization for room-temperature phosphorescence probing of 2,6-dichlorophenol, RSC Adv. 2015, 5, 19799.

[4] R.N. Liang, D.A. Song, R.M. Zhang, W. Qin, Potentiometric Sensing of Neutral Species Based on a Uniform-Sized Molecularly Imprinted Polymer as a Receptor,

Angew. Chem., Int. Ed. 2010, 49, 2556.

[5] S.F. Xu, L.X. Chen, J.H. Li, W. Qin, J. Ma, Preparation of hollow porous molecularly imprinted polymers and their applications to solid-phase extraction of triazines in soil samples, J. Mater. Chem. 2011, 21, 12047.

[6] J. Orozco, A. Cortes, G.Z. Cheng, S. Sattayasamitsathit, W. Gao, X.M. Feng, Y.F. Shen, J. Wang, Molecularly imprinted polymer-based catalytic micromotors for selective protein transport. J. Am.Chem. Soc. 2013, 135, 5336.

[7] G. Wulff, J. Liu, Design of Biomimetic Catalysts by Molecular Imprinting in Synthetic Polymers: The Role of Transition State Stabilization, Acc. Chem. Res. 2012, 45, 239.

[8] J.F. Yin, Y. Cui, G.L. Yang, H.L. Wang, Molecularly imprinted nanotubes for enantioselective drug delivery and controlled release, Chem. Commun. 2010, 46, 7688.

[9] G.J. Guan, R.Y. Liu, Q.S. Mei, Z.P. Zhang, Molecularly Imprinted Shells from Polymer and Xerogel Matrices on Polystyrene Colloidal Spheres, Chem. Eur. J. 2012, 18, 4692.

[10] J.D. Dai, X. Wei, Z.J. Cao, Z.P. Zhou, P. Yu, J.M. Pan, T.B. Zou, C.X. Li, Y.S. Yan, Highly-controllable imprinted polymer nanoshell at the surface of magnetic halloysite nanotubes for selective recognition and rapid adsorption of tetracycline, RSC Adv. 2014, 4, 7967.

[11] B.J. Gao, J. Wang, F.Q. An, Q. Liu, Molecular imprinted material prepared by novel surface imprinting technique for selective adsorption of pirimicarb, Polymer, 2008, 49, 1230.

[12] F.Q. An, B.J. Gao, X.Q. Feng, Adsorption and recognizing ability of molecular imprinted polymer MIP-PEI/SiO2 towards phenol, J. Hazard. Mater., 2008, 157, 286.

[13] L.G. Chen, J. Liu, Q.L. Zeng, H. Wang, A.M. Yu, H.Q. Zhang, L. Ding, Preparation of magnetic molecularly imprinted polymer for the separation of tetracycline antibiotics from egg and tissue samples, J. Chromatogr., A. 2009, 1216, 3710.

[14] X.Y. Liu, Y. Guan, X.B. Ding, Y.X. Peng, X.P. Long, X.C. Wang, K. Chang,

Design of temperature sensitive imprinted polymer hydrogels based on multiple-point hydrogen bonding, Macromol. Biosci. 2004, 4, 680.

[15] X. Wei, M.J. Meng, Z.L. Song, L. Gao, H.J. Li, J.D. Dai, Z.P. Zhou, C.X. Li, J.M. Pan, P. Yu, Y.S Yan, Synthesis of molecularly imprinted silica nanospheres embedded mercaptosuccinic acid-coated CdTe quantum dots for selective recognition of λ-cyhalothrin, J. Lumin. 2014, 153, 326.

[16] W. Zhang, W. Liu, P. Li, H.B. Xiao, H. Wang, B. Tang, A Fluorescence Nanosensor for Glycoproteins with Activity Based on the Molecularly Imprinted Spatial Structure of the Target and Boronate Affinity, Angew. Chem. Int. Ed. 2014, 53, 12489.

[17] H.L. Liu, G.Z. Fang, C.M. Li, M.F. Pan, C.C. Liu, C. Fan, S. Wang, Molecularly imprinted polymer on ionic liquid-modified CdSe/ZnS quantum dots for the highly selective and sensitive optosensing of tocopherol, J .Mater. Chem. 2012, 22, 19882.

[18] W. Zhang, X.W. He, Y. Chen, W.Y. Li, Y.K. Zhang, Composite of CdTe quantum dots and molecularly imprinted polymer as a sensing material for cytochrome c, Biosensors and Bioelectronics 2011, 26, 2553.

[19] X. Wei, Z.P. Zhou, T.F. Hao, H.J. Li, Y.Q. Xu, K. Lu, Y.L. Wu, J.D. Dai, J.M. Pan, Y.S. Yan, Highly-controllable imprinted polymer nanoshell at the surface of silica nanoparticles based room-temperature phosphorescence probe for detection of 2,4-dichlorophenol, Anal. Chim. Acta 2015, 870, 83.

[20] J.B. Liang, J.W. Liu, Q. Xie, S. Bai, W.C. Yu, Y.T. Qian, Hydrothermal growth and optical properties of doughnut-shaped ZnO microparticles, J. Phys. Chem. B 2005, 109, 9463.

[21] S. Hu, C. Xu, G. Wang, D. Cu, Voltammetric determination of 4-nitrophenol at a sodium montmorillonite-anthraquinone chemically modified glassy carbon electrode, Talanta 2001, 54, 115.

[22] H. Yin, Y. Zhou, R. Han, Y. Qiu, S. Ai, L. Zhu, Electrochemical oxidation behavior of 2,4-dinitrophenol at hydroxylapatite film-modified glassy carbon electrode and its determination in water samples, J. Solid. State. Electrochem. 2012, 16, 75.

[23] M.J. Thompson, L.N. Ballinger, S.E. Cross, M.S. Roberts, High-performance liquid chromatographic determination of phenol, 4-nitrophenol, β-naphthol and a number of their glucuronide and sulphate conjugates in organ perfusate, J. Chromatogr. B. 1996, 677, 117.

[24] X.F. Guo, Z.H. Wang, S.P. Zhou, The separation and determination of nitrophenol isomers by high-performance capillary zone electrophoresis, Talanta 2004, 64, 135.

[25] W. Huang, C. Yang, S. Zhang, Simultaneous determination of 2-nitrophenol and 4-nitrophenol based on the multi-wall carbon nanotubes nafion-modified electrode, Anal. Bioanal. Chem. 2003, 375, 703.

[26] S. Li, D. Du, J. Huang, H. Tu, Y. Yang, A. Zhang, One-step electrodeposition of a molecularly imprinting chitosan/phenyltrimethoxysilane/AuNPs hybrid film and its application in the selective determination of p-nitrophenol, Analyst 2013, 138, 2761.

[27] X. Liu, Y. Ji, Y. Zhang, H. Zhang, M. Liu, Oxidized multiwalled carbon nanotubes as a novel solid-phase microextraction fiber for determination of phenols in aqueous samples, Journal of Chromatography A 2007, 1165, 10.

[28] Y. Guo, X.B. Cao, X.M. Lan, C. Zhao, X.D. Xue, Y.Y. Song, Solution-based doping of manganese into colloidal ZnO nanorods, J. Phys. Chem. C, 2008, 112, 8832.

[29] C.B. Liu, Z.L. Song, J.M. Pan, Y.S. Yan, Z.J. Cao, X. Wei, L. Gao, J. Wang, J.D. Dai, M.J. Meng, P. Yu, A simple and sensitive surface molecularly imprinted polymers based fluorescence sensor for detection of λ-Cyhalothrin, Talanta 2014, 125, 14.

[30] K. Yoshimatsu, K. Reimhult, A. Krozer, K. Mosbach, K. Sode, L. Ye, Uniform molecularly imprinted microspheres and nanoparticles prepared by precipitation polymerization: The control of particle size suitable for different analytical applications, Anal. Chim. Acta 2007, 584, 112.

[31] S. Gam-Derouich, M.N. Nguyen, A. Madani, N. Maouche, P. Lang, C. Perruchot, M.M. Chehimi, Aryl diazonium salt surface chemistry and ATRP for the preparation of molecularly imprinted polymer grafts on gold substrates, Surf. Interface Anal. 2010, 42, 1050.

Tables

Table 1 Recovery of 4-NP in Yangtze River samples with 4-NP solution at different concentration levels (n= 5)

Sample	Concentration taken (μmol L^{-1})	Found (μmol L^{-1})	Recovery (%)	RSD (%)
1	0.5	0.469	93.8	5.6
2	1.0	1.053	105.3	4.7
3	2.0	2.062	103.1	3.7
4	4.0	3.904	97.6	3.1
5	8.0	7.896	98.7	4.3
6	12	12.104	100.87	2.8

Figures

Figure 1 Schematic illustration for the preparation of MIPs-ZnO NRs

Figure 2 TEM images of ZnO NRs with insufficient reaction time (36 hours) (a) and sufficient reaction time (72 hours) (b), TEM images(c) and High resolution TEM images (d) of MIPs-ZnO NRs.

Figure 3 SEM images of ZnO NRs and MIPs-ZnO NRs.

Figure 4 XRD pattern of MIPs-ZnO NRs. For a comparison, the XRD pattern of ZnO NRs was included (inset).

Figure 5 FT-IR spectra of KH-570-ZnO NRs (a; curve 1), ZnO NRs (a; curve 2), MIPs-ZnO NRs(b; curve 1) and NIPs-ZnO NRs(b; curve 2).

Figure 6 Effects of the concentration of MIPs-ZnO NRs on FL intensity. Curve a: the function of variation rate of FL intensity of detection system (containing MIPs-ZnO NRs + 4.0 μmol/L 4-NP) vs. concentration of MIPs-ZnO NRs; Curve b: the function of relative FL intensity vs. concentration of MIPs-ZnO NRs

Figure 7 Stabilities of MIPs-ZnO NRs (a) and Study of response time of 4-NP onto MIPs-ZnO NRs via FL detection (b).

Figure 8 FL emission spectra of MIPs-ZnO NRs (a) and NIPs-ZnO NRs (b) (12 mg/L) with addition of the indicated concentrations of 4-NP in water solution and the Stern−Volmer plots for MIPs-ZnO NRs (c) and NIPs-ZnO NRs (d).

Figure 9 Quenching amounts of MIPs-ZnO NRs and NIPs-ZnO NRs by different kinds of 10 μmol L^{-1} phenols (4-NP, 2,4-DCP, 2,6-DCP, 2,4,5-TCP).

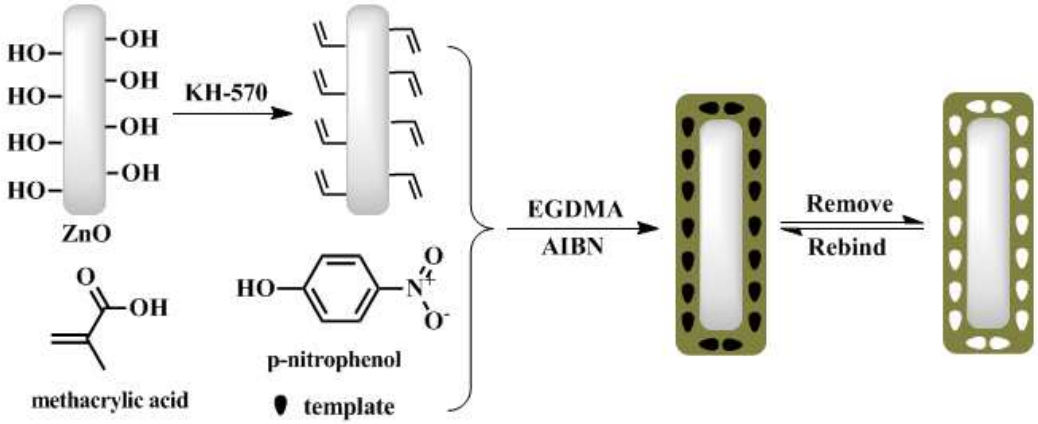

Figure 1 Schematic illustration for the preparation of MIPs-ZnO NRs

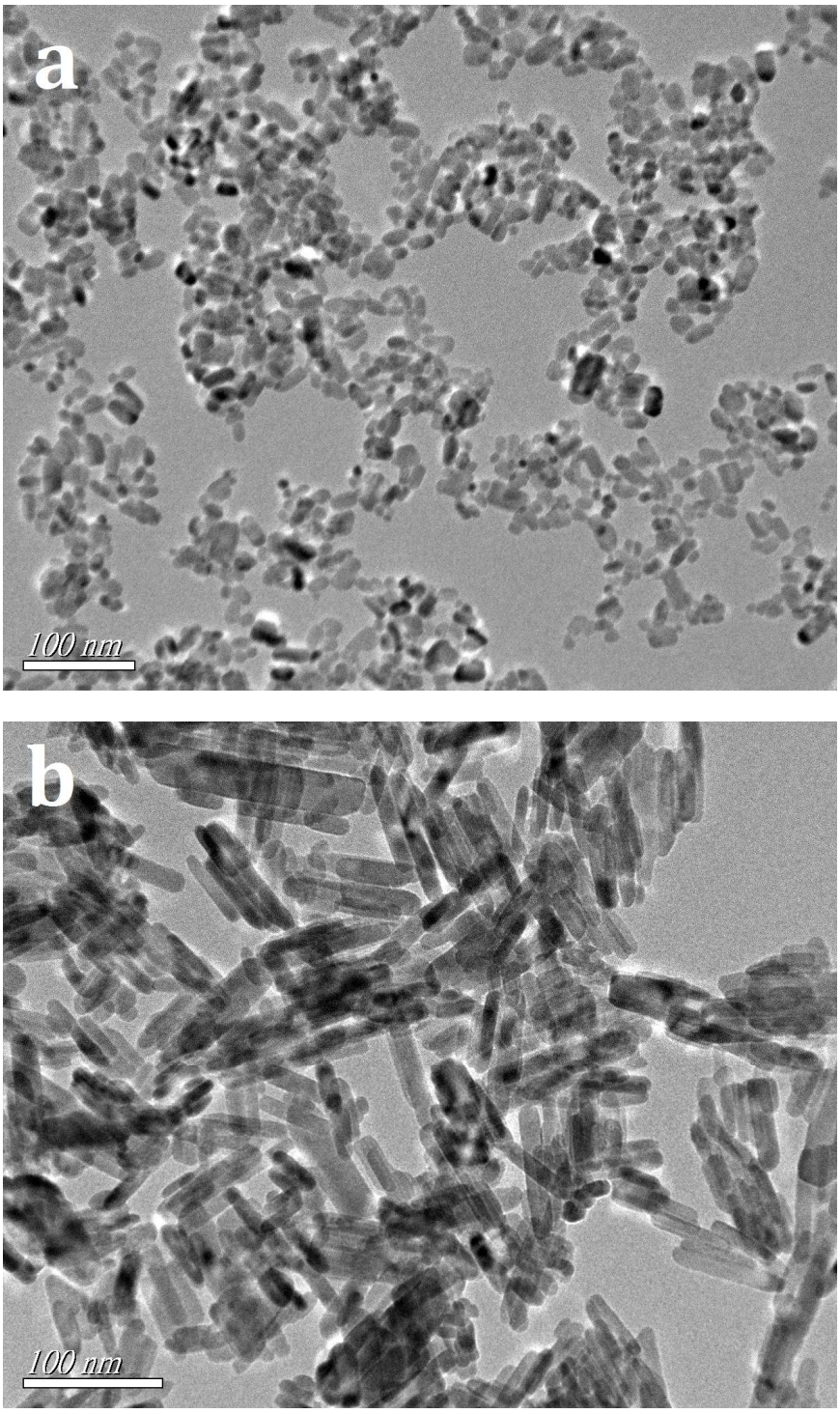

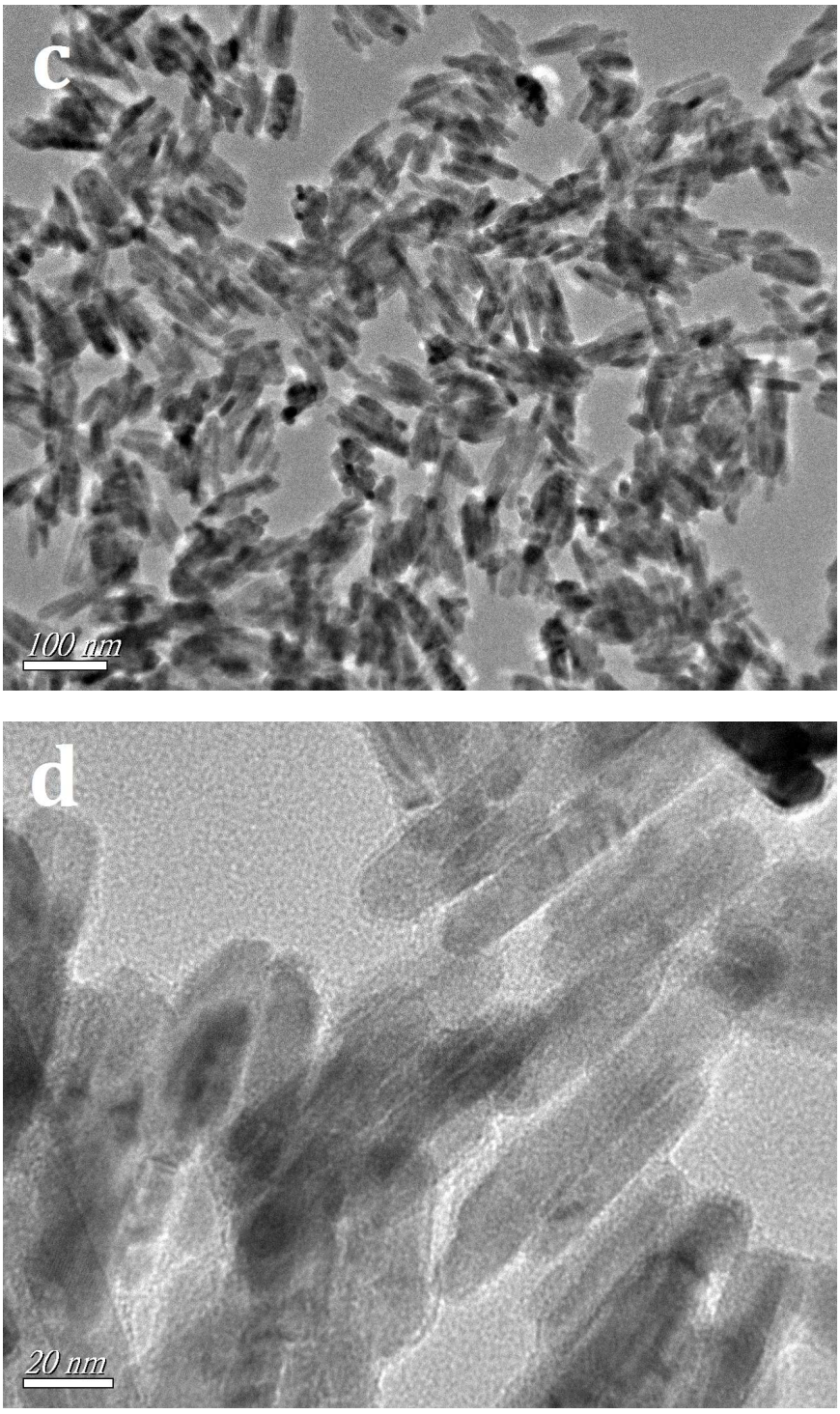

Figure 2 TEM images of ZnO NRs with insufficient reaction time (36 hours) (a) and sufficient reaction time (72 hours) (b), TEM images(c) and High resolution TEM images (d) of MIPs-ZnO NRs.

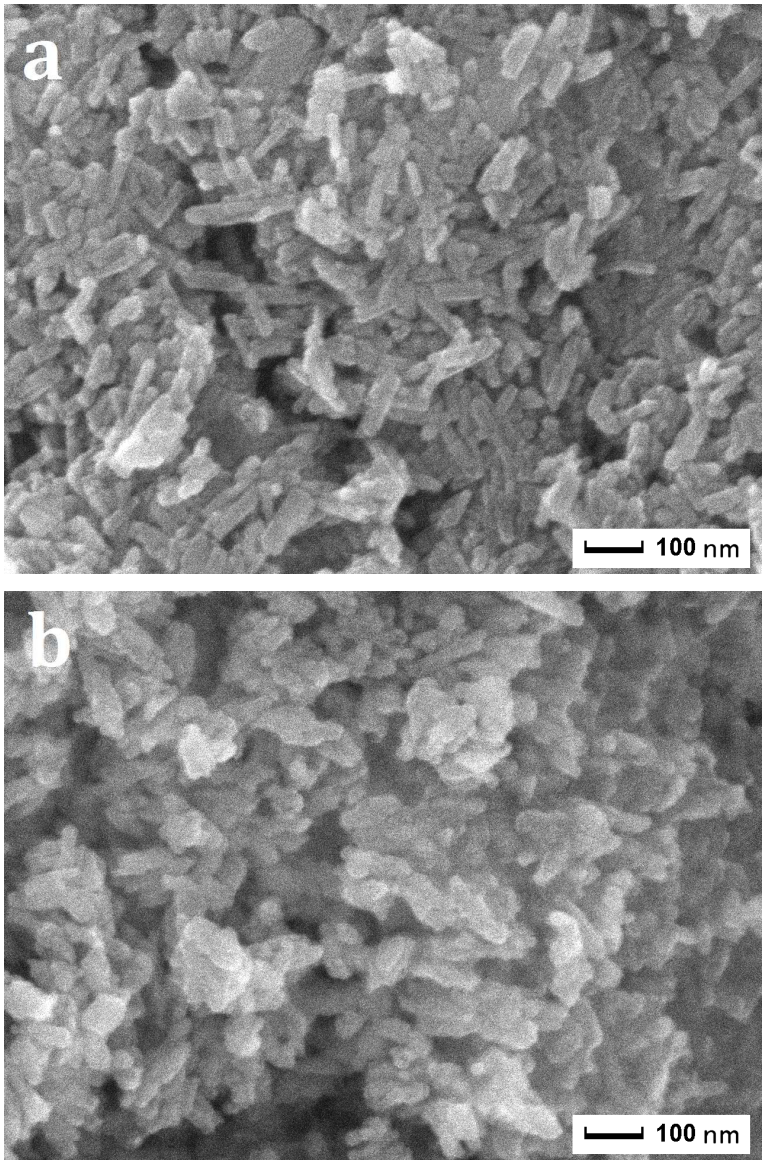

Figure 3 SEM images of ZnO NRs and MIPs-ZnO NRs.

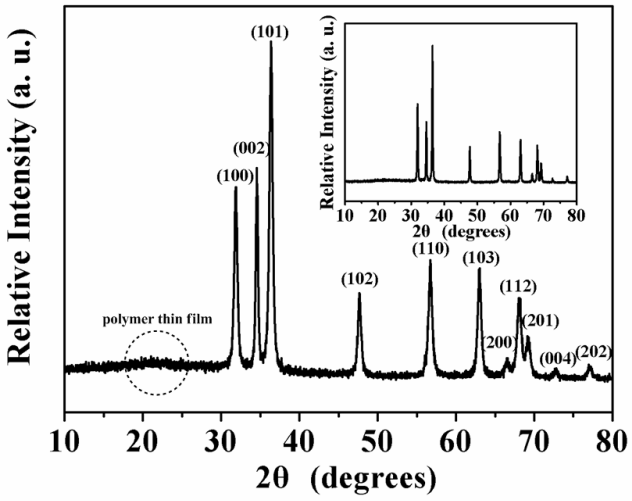

Figure 4 XRD pattern of MIPs-ZnO NRs. For a comparison, the XRD pattern of ZnO NRs was included (inset).

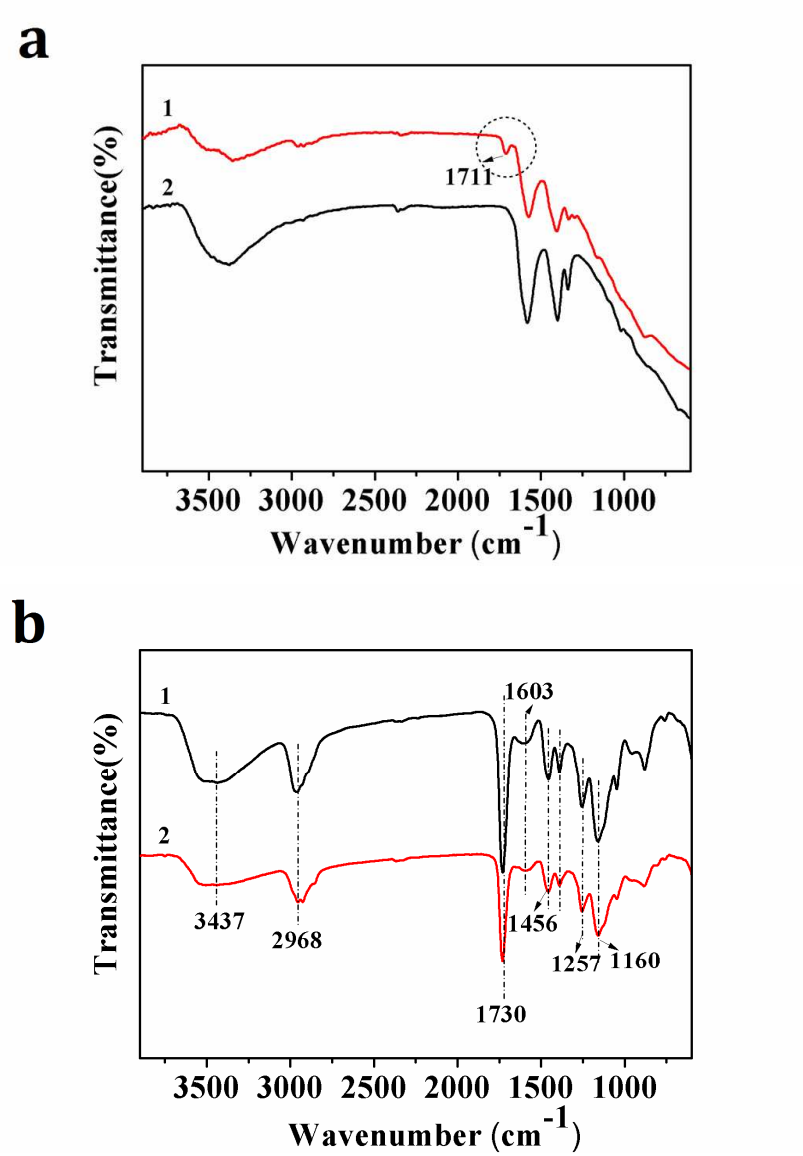

Figure 5 FT-IR spectra of KH-570-ZnO NRs (a; curve 1), ZnO NRs (a; curve 2), MIPs-ZnO NRs(b; curve 1) and NIPs-ZnO NRs(b; curve 2).

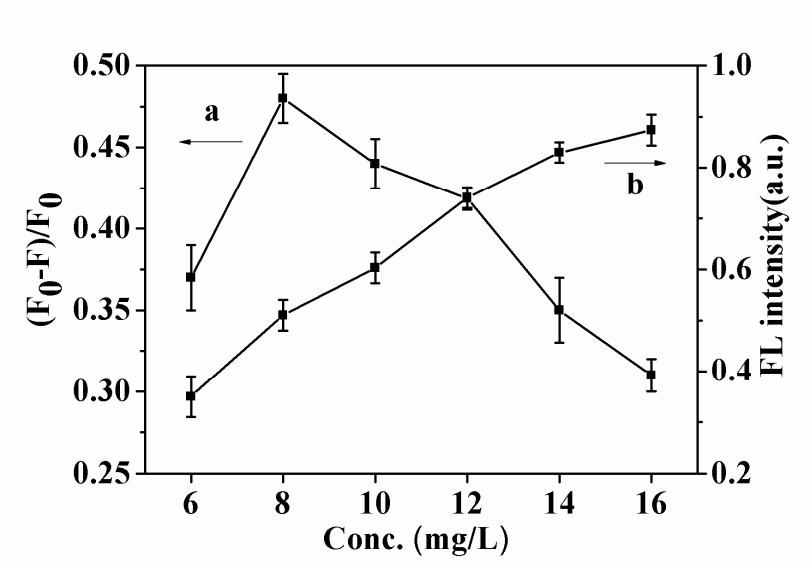

Figure 6 Effects of the concentration of MIPs-ZnO NRs on FL intensity. Curve a: the function of variation rate of FL intensity of detection system (containing MIPs-ZnO NRs + 4.0 μmol/L 4-NP) vs. concentration of MIPs-ZnO NRs; Curve b: the function of relative FL intensity vs. concentration of MIPs-ZnO NRs

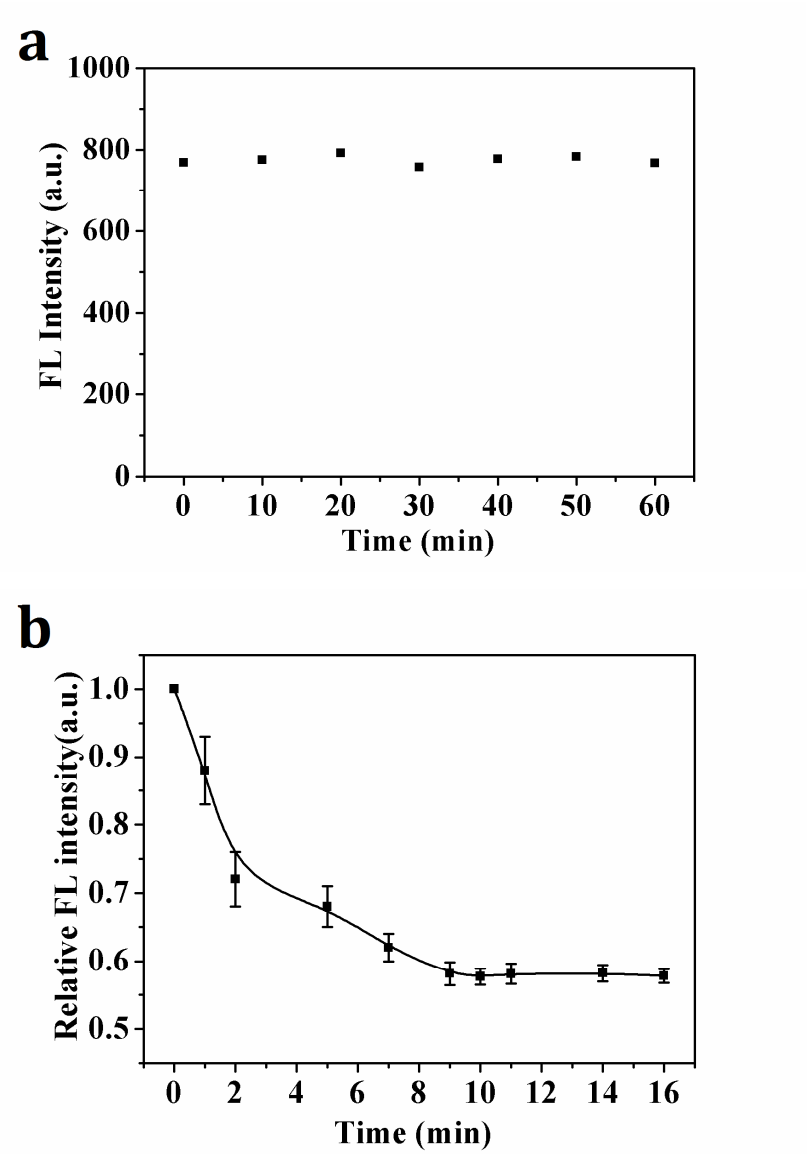

Figure 7 Stabilities of MIPs-ZnO NRs (a) and Study of response time of 4-NP onto MIPs-ZnO NRs via FL detection (b).

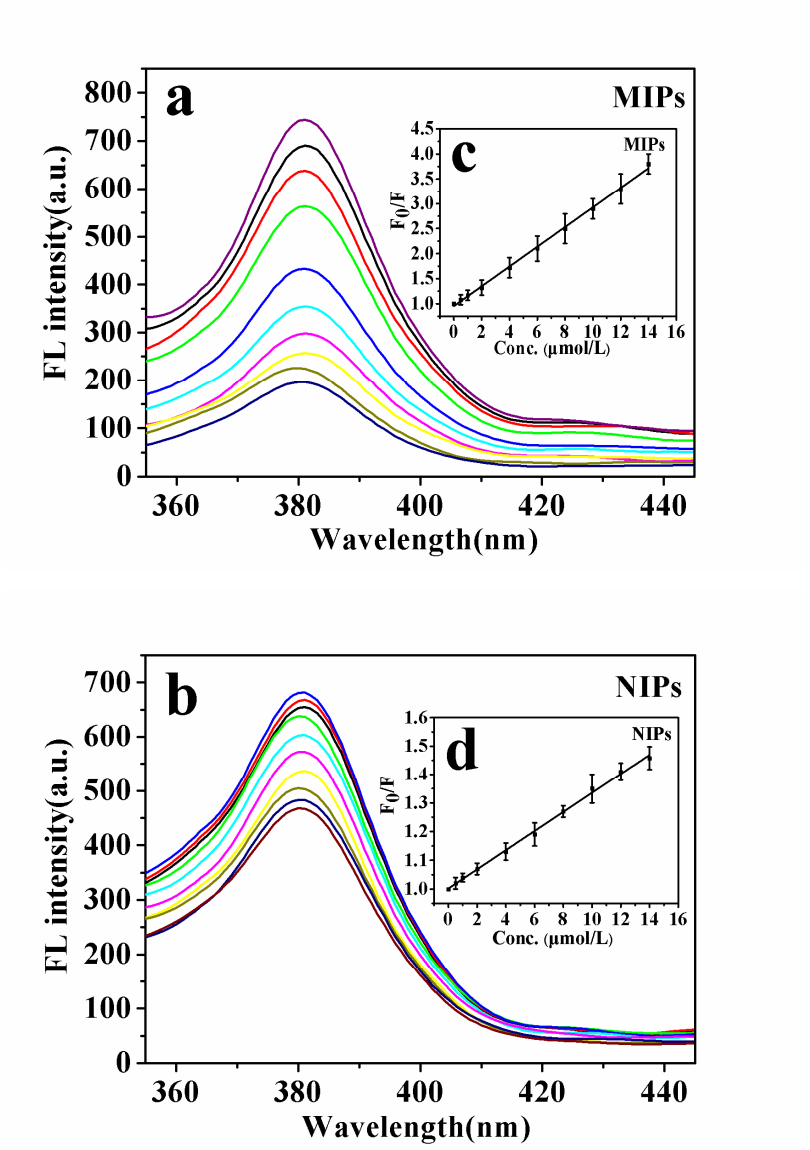

Figure 8 FL emission spectra of MIPs-ZnO NRs (a) and NIPs-ZnO NRs (b) (12 mg/L) with addition of the indicated concentrations of 4-NP in water solution and the Stern−Volmer plots for MIPs-ZnO NRs (c) and NIPs-ZnO NRs (d).

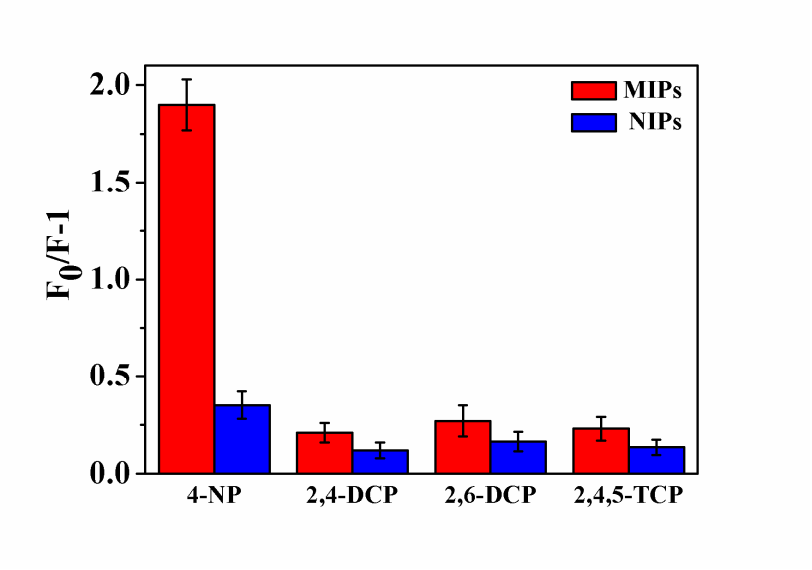

Figure 9 Quenching amounts of MIPs-ZnO NRs and NIPs-ZnO NRs by different kinds of 10 μmol L^{-1} phenols (4-NP, 2,4-DCP, 2,6-DCP, 2,4,5-TCP).